Ecole Doctorale
des Sciences
Physiques et de
l'Ingénieur

Master
Mécanique
et Ingénieries,
voie Recherche

université de BORDEAUX

Mémoire de Recherche

Session 2015-2016

Titre

Comportement thermo-rhéologique d'un mélange solide sulfate de calcium/eau soumis à des chargements thermiques isotropes sévères à la méso-échelle

Title

Thermo-Rheology kinetic of a solid mixture of Calcium Sulfate and water under isotropic severe thermal loading at mesoscale

Auteur

M. ALI ALBAHRANI

ENCADREMENT:

UNIVERSITE DE CERGY PONTOISE – UFR Sciences et Techniques

B. Ledésert, Pr. - Laboratoire Géosciences Environnement Cergy – GEC EA4506

R. Hébert, Dr. - Laboratoire Géosciences Environnement Cergy – GEC EA4506

Y.Melinge, Pr. - Laboratoire de Mécanique et Matériaux du Génie Civil – L2MGC EA4114

J. Eslami, Dr. - Laboratoire de Mécanique et Matériaux du Génie Civil – L2MGC EA4114

- ABSTRACT -

Thermo-rheology kinetic of a solid mixture of calcium sulfate and water under isotropic severe thermal loading is studied at mesoscale. The influence of water content ratio and heat rate on the thermal-rheological behavior of calcium sulfate and water (plaster) is investigated. Thermal dilatometer tests are performed on three different water to plaster mass ratios cylindrical samples (11mm height and 8mm diameter) at six different heat rates (1, 3, 5, 20 and 50°C/min). Temperature gradient is investigated in thermocouples tests indicating mass transfer. Zones of mass transfer and phases changes are analyzed. Thermo-rheological behavior general representation using master curves is mentioned at the end along with a chemical modification is tested for potential improvement.

- RESUME -

Dans ce projet de recherche, quelques aspects de cinétiques thermo-rhéologiques d'un mélange solide de sulfate de calcium et d'eau eau soumis à des chargements thermiques isotropes sévères sont étudiés à la méso-échelle. L'influence de la teneur en eau et de la vitesse de chauffe est particulièrement étudiée. A cette fin, des essais dilatométriques thermiques sont effectués pour trois rapports E/P (rapport de la masse d'eau et de la masse de platre) différents et six vitesses de chauffe différentes (1, 3, 5, 20 et 50°C/min). Les échantillons étudiés sont cylindriques et de dimensions suffisantes pour une bonne représentation du milieu poreux (hauteur de 11 mm et 8 mm de diamètre). L'existence d'un gradient de température est étudiée en ayant recours à l'instrumentation des échantillons. Le protocole d'essais renseigne le transfert de masse au cours de la phase de déshydratation. Les zones de transfert de masse et de changements de phases chimiques sont analysées. Une tentative de représentation globale de l'influence de la température est finalement proposée via une courbe maîtresse. Avec l'objectif d'améliorer les propriétés de contraction du mélange initial, des perspectives sont avancées en introduisant un additif minéral au mélange plâtre-eau.

TABLE OF CONTENTS

LIST OF SYMBOLS

PL:	plaster	
PLF:	plaster and silica fume	
W/P:	water to plaster mass ratio	(-)
ΔL/L0:	dilatation	(-)
R^2:	linear regression coefficient	(-)
β_T:	thermal expansion coefficient	1/°C
β:	heat rate	°C/min
Tc:	critical temperature	°C
T_dilato:	temperature readings from the dilatometer	°C
T_thermo:	temperature readings from thermocouples	°C
ΔT:	temperature deference between skin and center of the sample	°C
$\partial T/\partial r$:	temperature gradient	°C/m
t*:	experimental (measured) time	s
t:	estimated (calculated) time	s
Q:	quantity of heat transferred to or from the object	J
m:	mass	g
ρ:	density	g/m^3
C*p*:	specific heat	J/k
λ:	thermal conductivity	W/km
ε:	porosity	(-)
RH:	relative humidity	(-)
THCM:	thermal, hydrous, chemical and mechanical behavior	
TGA:	thermal gravimetric analysis	
TDA:	thermal deferential analysis	
SEM:	scanning electron microscope	
ESEM:	environmental scanning electron microscopy	
Fig:	figure	

INTRODUCTION

Since ancient times, gypsum has been used as finishing material for walls and ceilings in many countries. Its excellent performance attractive appearance, easy application, and its healthful contribution to living conditions have made gypsum a most popular finishing material for these applications [1]. In addition, the large availability, relative low cost, easy handling and mechanical characteristics suitable for different uses, makes the gypsum a widely used construction material [2]. However, gypsum presents some undesirable characteristics, as brittleness and weakness in tension, coupled with high water solubility, hindering outdoor application. The global production of gypsum in 2008 is over 250 million ton. Taking Europe as an example, there are 160 quarries for gypsum production with number of employees over 28,000 [3]. Calcium sulfate occurs in nature as a mineral gypsum, i.e. calcium sulfate dihydrate CaSO4·2H2O, or in the anhydrous form called anhydrite [4]. If mineral gypsum is heated, it partially loses water and at the temperature of 120°C-130°C transforms into the calcined gypsum (commonly known as hemihydrate or plaster of Paris) CaSO4·0,5H2O, which easily takes water and then hardens. If heating process is continued, the material turns into anhydrous calcium sulfate. The occurring transformations are accompanied by changes in crystal structure of the material and related changes in its density. In the field of construction, buildings must be able to withstand accidents, natural or otherwise, that may occur during their lifetime. To minimize the impact of these incidents, the choice of building materials is paramount. For a fire protection, a set of elements of protection is in place to facilitate the evacuation of people, to limit the spread of fire and facilitate the intervention of emergency.

We distinguish passive protection and active protection. The *active protections* are represented by the fire detection systems implemented to facilitate the evacuation of the premises and the emergency services. The p*assive protection* is directly related to the behavior of the structure. The materials dedicated to fire protection are composed mainly of latent heat in materials and/or low thermal conductivity. This is why the plaster is widely used in fire protection. Indeed, besides being a phase change material, it has a low thermal conductivity. Combining these two properties provides the delay spread of the temperature. However, the plaster has low mechanical properties, which is why it is not used as a structural member. Most often, it is reinforced with fibers and/or minerals [5]. Calcium sulfate hemihydrate is extensively used in buildings, ceramics and medical industries. Hydration of hemihydrate is a highly exothermic reaction and occurs as equation 1 shows:

$$CaSO_4 \cdot 2H_2O + Q \rightarrow CaSO_4 \cdot 0.5H_2O + 1.5H_2O \quad \text{(Eq.1)}$$

Where Q is the amount of heat evolved depends on number of factors. During hydration, gypsum crystallization takes place, however, when the hydration occurs in pastes, the plaster sets and develops strength [6]. With the aim to better model the THCM behavior of building macro system submitted to fire (part of protected structures, ceiling, smoke exhaust ducts, ventilation ducts, specific equipment's etc), the present project is devoted to the shrinkage study of gypsum materials during temperature evolution. Due to the poor information in the literature, the thermo strain is studied taken into account the influence of the temperature, the heat rate and the water to plaster ratio. Tests at intermediate scale are carried out to ensure a good representation of the porous media. Plus, the expected results could help us to analyze the effects of the material chemical changes already identified at micro scale.

The report is presented as follow: First chapter (Ch.I) dedicated for literature review on plaster and thermal, hydrous, chemical and mechanical behavior (THCM) along with defining the faire case conditions that governed this study. Followed by chapter two (Ch.II) which presents the objective of the project. Methodologies, used material and devices are introduced in the third chapter. Chapter four (Ch.IV) presents all the results and analysis. Last chapter is about improvement in the rheological behavior. Finally, the main conclusion is presented.

Ch.I) LITERATURE

a. Plaster

The plaster is obtained from gypsum. Plaster and mineral have the same chemical formula CaSO4.2H2O. However, the microstructure is different. Plaster is a calcium sulfate dihydrate ($CaSO_4.2H_2O$) which is obtained by mixing anhydrous calcium sulfate (CaSO4) or hemihydrate ($CaSO_4.0{,}5H_2O$) and water. Calcium sulfate and hemihydrate are obtained by heat treatment of gypsum. Gypsum is a mineral of natural origin (plaster stone) or synthetic Fig.1. The word plaster refers to both the plaster powder and also to the finished product. We denote in this study by the term "plaster" the rehydration product also called set plaster [5].

Fig.1 Photography of crystals of natural gypsum - *FigI-4 in [5]* -

$CaSO_4$ / H_2O system consists in five crystalline phases: the gypsum, hemihydrate, anhydrite III, anhydrite II and anhydrite I. The phase changes within the system depend on the conditions of temperature and pressure. Gypsum crystals develop various morphologies: tabular, fibrous, sugary, lenticular, dependent on growing conditions. The industrial dehydration and rehydration of different calcium sulfates are shown in Fig.2. Bezou in his thesis [7] was able to show the existence of two sub-hydrates, one with 0.5 molecule of water and the other 0.6. The other measured quantities would simply due to water absorbed by the structure through its metastability. Calcium sulfate is often called hemihydrate (CaSO4.0,5H2O). Depending on the process of industrial production, hemihydrate occurs in two different forms (α- and β-forms); α-form is prepared by wet method (e.g., autoclaving) and β-form is prepared by dry methods (e.g., calcining) from calcium sulfate dihydrate [6]. In the laboratory βhemihydrate is prepared from the dihydrate by heating under a low water vapor partial pressure, i.e., in dry air or vacuum, between 45°C and 200°C whereas α hemihydrate is prepared from the dihydrate under a high partial pressure of water vapor, e.g., above 45°C in acid or salt solutions, or above 97.2ºC in water under pressure. Lehmann [8] carried out differential thermal analysis of both the forms and found differences in the transformation temperatures. According to Follner et al. [9], there are differences in the structures of the two forms of hemihydrate but the structures are difficult to establish. Scanning electron microscopy pictures Fig.3 have shown that the α-hemihydrate consists of well-formed transparent idiomorphic crystals with sharp crystal edges whereas β-hemihydrate consists of flaky particles made up of small crystals. β-hemihydrate requires more water than the α-hemihydrate in order to obtain a paste of standard consistency because it has a much higher specific surface area [6].

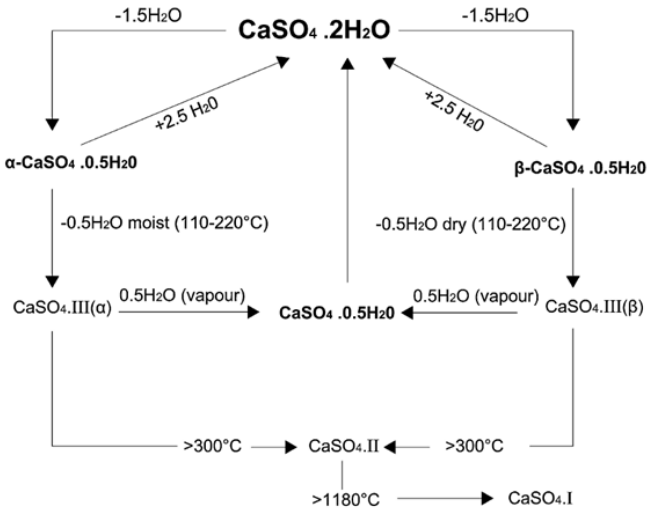

Fig.2 Industrial dehydration and rehydration calcium sulfates *-Fig.1 in [6]-*

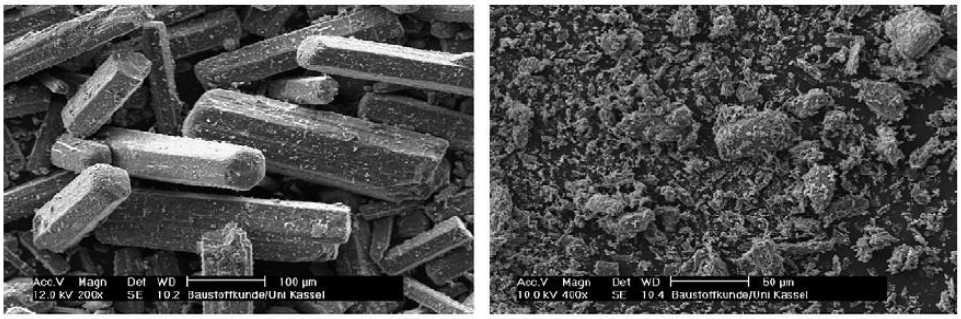

SEM of α-hemihydrate SEM of β-hemihydrate

Fig.3 Scanning Electron Microscopic (SEM) of the two forms of hemihydrates -*Fig.3 in [6]*-

Anhydrite III crystallizes in the hexagonal system. It is an anhydrous calcium sulfate and very easily rehydrating. It's the reason why it has long been confused with the hemihydrate and not considered an own phase by the proximity of the two structures. Its existence and structure were unequivocally identified by Bezou [7] so various studies have been undertaken thereafter. Anhydrite II crystallizes in an orthorhombic system. It is a dry phase does not rehydrate or at least not spontaneously in air and exists as a plaster in nature. The crystals mainly adopt a tabular and prismatic morphology its stability explains that many studies are devoted to it. Anhydrite I is the high temperature phase of $CaSO_4/H_2O$ system. This phase is stable at temperatures above 1150°C, which explains the lack of interest in it. Anhydrite I could be identified as a phase crystallizing in a cubic system. Little additional information is present in the literature [5].

b. Thermal, hydrous, chemical and mechanical behavior (THCM)

Many studies focusing on the characterization of gypsum materials and properties which are presented in the literature, they characterize a wide range of materials by techniques various analyses [5]. This paper focuses on the identification of the following parameters: phase changes, mass transfer, dimensional variations, porosity and mechanical strength for plaster samples with different water to plaster mass ratio. These parameters represent the behavior of (THCM), which is very essential to better understand the material in order to characterize it and improve its properties under thermal loading.

Several methods are available to improve the chemical/mechanical properties of plaster. Chemically silica fume can be added in the plaster mixture. Mechanically fibers can be added. The main drawback in the use of natural fibers as reinforcement in composite materials is the weak interaction between fibers and matrix. Therefore, many studies were carried out on suitable chemical treatments on fibers to improve the adhesion between fiber and matrix, in order to increase the composite strength. Mechanical and technological properties can be controlled by adding the following substances [10]

- Asbestos, glass fiber – improves strength.
- Clay – increase cohesiveness, influence the material bonding time and increase permeability.
- Cement – allow for controlling changes in the coefficient of thermal expansion of the material.
- Silica flour, talc, silica sand – modify the volume changes during the bonding process. They reduce the content of plaster in the material thus influencing mainly the technological properties.

Thermal analyses are often used to highlight the properties of the material chemical changes. Thermo gravimetric analysis (TGA), Thermo differential analysis (TDA) are used to carry out the tests. TGA and TDA of a gypsum sample were performed in previous study in the work of A. ROJO [5], the aim was to check if there was any weight loss at the concerned temperatures, between 750°C and 900°C. Only two phenomena were observed during the TGA/TDA experiment. The first one corresponded to the dehydration

of gypsum between 100°C and 200°C, involving two reactions (dihydrate to hemihydrate and hemihydrate to anhydrite III). The second weight loss observed started at around 1250°C. It corresponded to the decomposition of anhydrite I into CaO, leading to a theoretical weight loss of 59% assumed that the reaction temperature was 1250°C [11]. It has to be noticed that there was no weight loss that could indicate a decomposition of the sample in the range of temperature where the phenomenon of crystal degradation was observed [12]. The starting sample consisting in dihydrate and hemihydrate was entirely transformed into hexagonal anhydrite (III) at the 150°C scan. It then changed to orthorhombic anhydrite (II) between the 225 and the 500°C scans. No phase transformation was then undergone until 1200°C when CaO started to appear [12].

The mass monitoring is mainly used on samples crushed to powder, using thermal gravimetric analysis TGA. of discontinuous measurements tests on bulk samples are also realized by thermal stabilization. For all materials studied by TGA, the weight decreases for temperatures between 80°C and 250°C. This loss is due to the dehydration of gypsum is transformed into anhydrite III and provides access to material purity. For materials consisting only of gypsum, this loss is 21.6%. The gypsum content of the various materials investigated is between 62% and 98%. In fact, they contain impurities and many additions, which is why other mass losses at higher temperature is observed [5]. The reaction temperature range is dependent on heat rate (β) and the initial mass. In addition, some studies suspect the effect of the saturation vapor pressure in the measuring cell that would tend to retard the loss of mass.

Regarding dilatometry $\Delta L/L_0$, the thermo-mechanical behavior of gypsum is investigated by Thermal dilatometric analysis (TDA) and discontinuous measurements of dimensional changes. Continuous measurements are performed under constant heating rates. A. ROJO [5] noted the effect of heat rate on TDA measures. At higher heat rate, the dilatometric phenomena are moved to higher temperatures. The measurements made for heat rates -between 5°C/min and 10°C/min- have a similar behavior for all the materials to a temperature of 400°C. Gypsum expands initially at temperatures up to 120°C. Various withdrawals are then observed. Between 120°C and 200°C, a shrinkage of less than 0.5% is induced by dehydration of gypsum. Between 350°C and 450°C, higher shrinkage is observed (between 1% and 3%). This is due to the phase change of the anhydrite III anhydrite II [5]. At higher temperatures, the material continues to contract. The observed removal is strongly dependent on the composition of the material can vary from 1 to 6%. For temperatures above 850°C, the materials undergo a sudden withdrawal of up to 20%. This withdrawal seems less important and appears at higher temperatures for the materials for fire protection. These dimensional changes eventually lead to the disintegration of the material [5].

Thermal Conductivity λ at room temperature the thermal conductivity values range between 0.14 and 0.56 W/Km. This heterogeneity at room temperature has several origins. All the material has a different chemical composition which affects the value of thermal conductivity. In addition, the materials are not all kept in the same conditions which changes the amount of water saturation in the gypsum matrix and therefore the initial thermal conductivity as could be seen in the work of Quénard [13]. At room temperature, the more the material is saturated with water, the higher its thermal conductivity will be.

The porosity (ε) at ambient temperature is a controlled value because it is directly related to mechanical strength of the material and mass transfer properties. Although, its evolution with temperature is unknown, few studies have reported an increase in porosity of 16% to 20% after drying of the material [14].

Plaster is a permeable material, yet its permeability rarely measured. The measured air permeability values have the same order of magnitude 10^{-14} m^2. The differences between measurements are due to the difference in composition and heterogeneities of the material, because used materials are usually not pure, they have impurities in the composition. For example, Shepel *et al.* [14] showed that paper impurities are less permeable

compared to plaster, which decrease the value of the permeability of the material. When the gypsum is heated, after drying, permeability increases. This phenomenon is due to the dehydration of gypsum inducing an increase in the porosity and therefore the permeability [5].

c. Fire case conditions

The interest of this project is on building fires defined by the standard relationship ISO 834 which is presented mathematically by Eq.2 and the standard ISO 834 fire curve shown in Fig.5. T is the temperature in °C, T_0 is the initial temperature in °C and t is the time in minutes.

$$T = T_0 + 345 \log(8t+1) \quad \text{(Eq.2)}$$

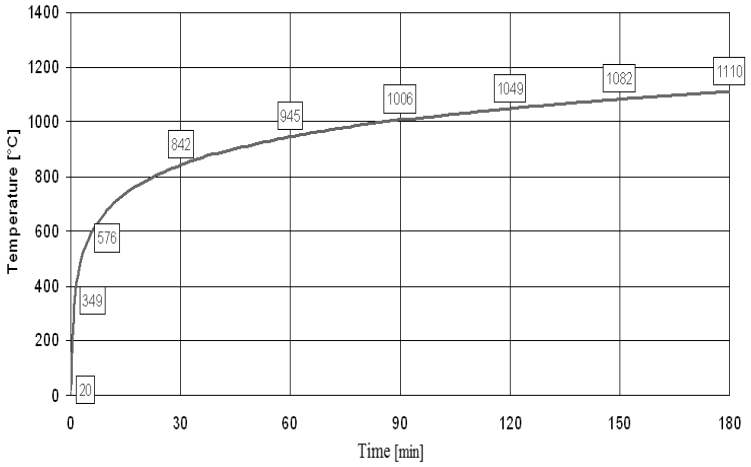

Fig.5 Standard ISO 834 fire curve *-modified from [15]-*

When the gypsum is subjected to a temperature rise, it is subjected to different phase changes which have been identified by X-ray and neutron temperature dependent. All of this work highlighted the dehydration of gypsum hemihydrate, for temperatures between 80°C-150°C followed by anhydrite III to temperatures ranging from 110°C to 250°C. For studies in temperature below 700°C, the last change of phase is observed the processing of the chemical change of anhydrite III anhydrite II that takes place between 300°C and 400°C.

Ch.II) OBJECTIVE OF THE PROJECT

This study is part of understanding the thermal, hydrous, chemical and mechanical behavior (THCM) of building materials submitted severe thermal loading like in a fire case. The Calcium Sulfate based materials are selected for this project. These materials are typical passive protection systems of structures in case of fire -standard curve ISO 834- by combining the effects of phase changes and good thermal insulation.

In previous work, we have shown many results to better understand the damage [5] and plan to continue the work by completing the characterization of phase changes at the microscopic level by a study of the thermo-rheological behavior in mesoscopic scale. Such work should enable us to interpret some kinetic structuring of the material to the macro scale. To this end, we are targeting the following phase changes during heating; decomposition of gypsum into anhydrite III via hemihydrate phase, which is accompanied by a behavioral porous expanding-contracting medium. Decomposition of anhydrite II and III characterized by a contracting behavior. Decomposition of calcite present naturally in the deposit exploited for the production of calcium sulfate and characterized by a contracting behavior.

During this project, the first part of the work was dedicated to literature to identify the results already available vis-à-vis literature thermo-rheological behavior. The second part, from samples representative of the microstructure and average porous medium, the study of thermal deformation is conducted using a thermal dilatometer with a protocol isotropic non-isothermal heating. The case of a linear heating over time will be selected by adjusting the heating rate between 1°C/min and 50°C/min. This project should characterize the repeatable nature of the rheological behavior and lead to the establishment of a pattern of behavior linked to phase changes of properties.

In the last part, a general rheological representation will be integrated using master curves.

Ch.III) METHODOLOGY, USED MATERIAL AND DEVICES

a. Used Material

The commercial β-hemihydrate (plaster β Extha Iberica) is used for this project. Hemihydrate is the major phase in plaster. Other phases are also present in small amounts such as calcite ($CaCO_3$), quartz (SiO_2) or dolomite ($CaMg(CO_3)_2$). These minerals are impurities frequently present in the ores of gypsum and therefore in their dehydration products. Average chemical composition of the hemihydrate is presented in Table.1. SEM photographs of the samples used are taken and presented in Fig.6. The observed size and morphology of crystals observed confirm the nature of the hemihydrate.

		Hémihydrate
Gypse	$CaSO_4.2H_2O$	
Hémihydrate	$CaSO_4.0{,}5H_2O$	$90{,}0 \pm 1{,}5$
Calcite	$CaCO_3$	$4{,}6 \pm 0{,}5$
Quartz	SiO_2	Trace
Dolomite		Trace

Table.1. Average chemical composition of the hemihydrate -*Table.III-1 in [5]*-

Fig.6 SEM images of the hemihydrate of samples of 0.66 water to plaster ratio before testing.

b. Samples preparation and general material properties

Cylindrical shaped samples were used in this project. 11mm height and 8mm diameter. 100 g of gypsum powder were mixed with different water contents (56g, 66g and 76g) in order to have water to plaster ratios (W/P) of 0.56, 0.66 and 0.76. Around one hundred samples were made for each W/P. After mixing the gypsum powder with water the outcome plaster mixture was poured into molds with specific mentioned dimensions. After around thirty minutes the mixture solidify and were extracted from the molds and placed in a drying chamber with constant ambient temperature to dry for ten to fourteen days at 20°C in temperature and 50% RH (relative humidity). Table.2 present the sample's mass used in this project regarding water to plaster ratio.

W/P	0.56	0.66	0.76
Mass	0.69g ± 0.01g	0.66g ± 0.01g	0.61g ± 0.01g

Table.2 Mass used for each water to plaster ratio

Plaster with silica fume samples were fabricated with 0.66 W/P ratio (70g Plaster, 30g silica fume and 66g water). The mass evolution of the samples of 0.66 W/P inside the drying chamber were observed over ten days for plaster and plaster with silica fume see Fig.7 and Fig.8. Mass samples reach a constant and repetitive value before thermal testing.

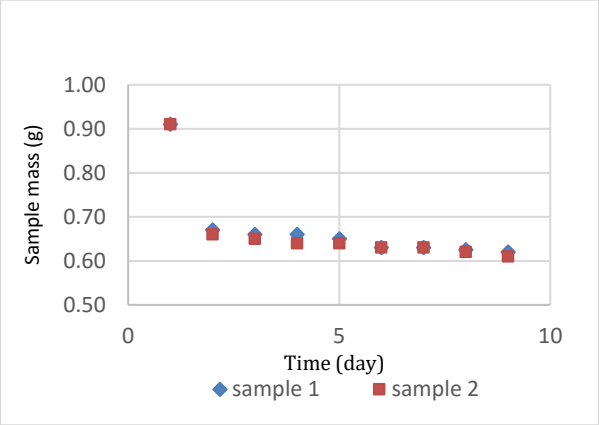

Fig.7 Mass evolution of plaster with w/p: 0.66

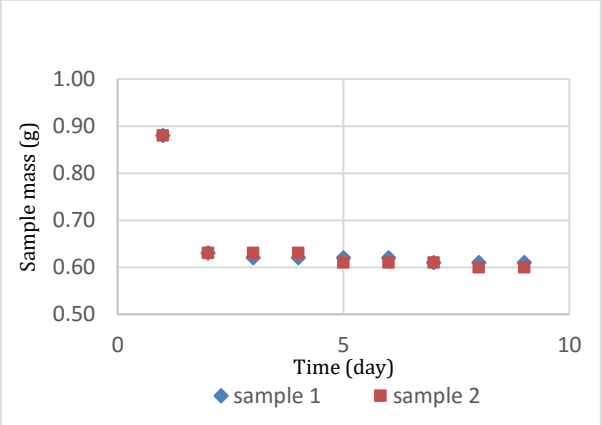

Fig.8 Mass evolution of plaster silica fume with w/p:0.66

c. Thermo-dilatometer Test

The dilatometer used is NETZSCH DIL 402 PC with a maximum temperature of 1100ºC, Fig.9 present the device with a schematic of its parts. In this project the studied temperature is ranged from 25ºC to 1000ºC and tests are done for six different heat rates; 1, 3, 5, 10, 20 and 50ºC/min. Calibration of apparatus is done each heat rate before testing the samples. All tests are repeated two times for each heat rate on each W/P ratio of the samples. When the temperature reaches 1000ºC the dilatometer stops automatically and kept closed for cooling process until around 25 ºC.

Fig.9 NETZSCH dilatometer (left) and a schematic of the main parts (right)

d. Instrumented thermal tests

Thermocouples of type S were installed at the center of some samples in the fabrication process to test the temperature deference between the border and the center of a sample in different heat rates. Tests were done for W/P ratio of 0.66 only on all heat rates (1, 3, 5, 10, 20 and 50ºC/min) with two times repetition. The outcome data extracted from thermocouples was compared with the data from dilatometer.

e. Experimental protocol

Plaster (PL)

Plaster of 0.66 W/P was selected to be the main testing series and the other water to plaster ratios were tested to study the effect of the water inside the mixture. Dried samples placed inside the dilatometer where six different samples are tested for each heat rate. The cooling process took in average five hours to cool from 1000ºC to room temperature. The test is repeated two times *(first test referred to as ESS and two repetitions referred to as Rep01 and Rep02).* Plaster of 0.75 and 0.56 W/P are tested by the same process and each is repeated one time *(first test referred to as ESS and one repetition referred to as Rep01).*

Instrumented Plaster with Thermocouples

With the aim to highlight the effect of the material temperature gradient (Which can be mainly explain the average shrinkage of the porous media) instrumented samples has been delivered. Plaster samples of 0.66 W/P are instrumented with thermocouples (type S) in the fabrication process. Dried samples are placed inside the dilatometer with the dilatation indicator (push rode) disconnected. Thermocouples are connected to another PC to record the data. The software of the thermocouples was started before launching the dilatometer. At the end two data sheet are needed, one from the thermocouple which recorded the temperature at the center of the sample and the other one is for the external temperature (Edge sample's temperature). The test is repeated one time *(first test ESS and one repetition Rep01).*

Plaster with silica fume

Plaster and silica fume samples of 0.66 W/P and silica fume to plaster mass ratio is 0.3. Such addition is retained to increase the data bank already created by A. ROJO (2013) [5]. Dried samples placed inside the dilatometer where six different samples were tested for each heat rate. The test was repeated one time *(first test ESS and one repetition Rep01).*

Ch.IV) RESULTS AND ANALYSIS

a. Thermo rheological behavior

A general look on the dilatation behavior of plaster is shown in Fig.10. The plot is divided by zones regarding temperature. It consists of two main parts; *dilation* and *contraction*.

- In zone 1, the thermo strain is not significant. A temperature yield must be reached to clearly observe a strain.
- In zone 2, the thermo strain versus the temperature evolution shows a dilatation process. This behavior is logically governed by the water content. Such behavior reaches a maximum corresponding to the overtaking of the thermal barrier. Dehydration chemical change is started.
- Zone 3. After the observed maximum, contraction of the material is observed. Such a rheological behavior is combined with the water molecule release.
- Zone 4 is the limit of irreversibility and zone 5 is the period of reorganizing the system's crystals transforming Anhydrite III to Anhydrite II.
- In zone 6, 7 and 8, the contraction seems to be in accordance with the chemical change of the Anhydrite II. But such a contraction is clearly combined with the dilatation of the CO_2 release during the chemical change of the calcite.

Such result is quite similar to those already presented in the literature, except the zone 7 induced by the presence of the calcite in the material. Plus, those macro strain behaviors are clearly in accordance with the crystals changes and already observed at micro scale, A. ROJO (2013) [5]. Phase changes is influenced by the temperature, because of interaction of plaster in case of fire plays a role with the speed of heat *(heat rate)* on thermo rheological behavior. Porosity calculated before testing versus water content ratio is presented in Table.3.

W/P	0.56	0.66	0.76
porosity (ε)	0.46	0.52	0.56

Table.3 Porosity value by water to plaster ratio

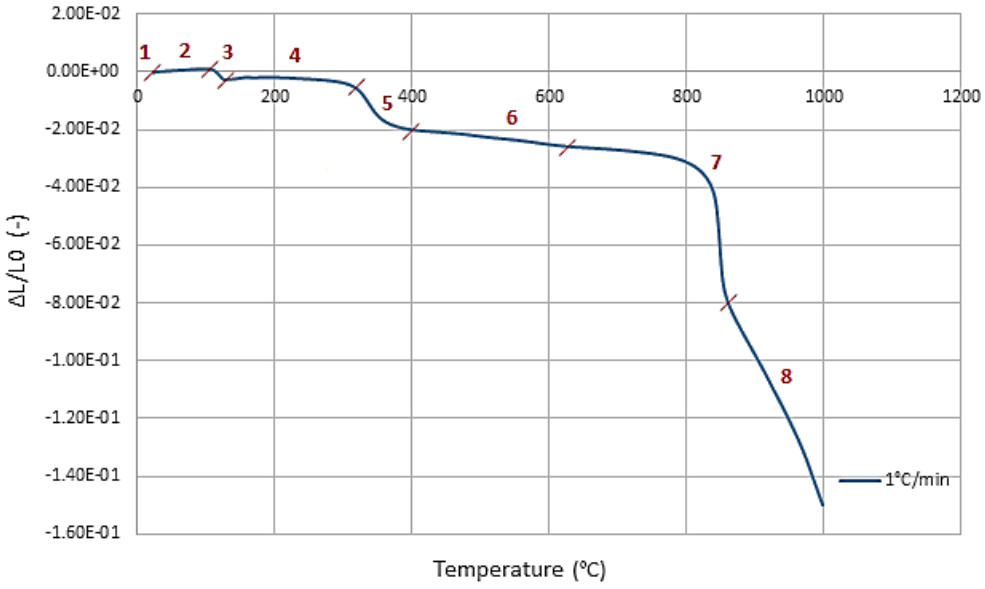

Fig.10 General behavior of plaster in dilatometer test of 1°C/min.

In this section, the main zones identified in Fig.10 and their associated parameters are analyzed.

b. Analysis of zone 2

The starting temperature of the zone 2 *(critical temperature)* is firstly analyzed. The influence of the water content and the heat rate is presented in the Fig.12. Due to quality of the presented results, an average critical temperature (avg Tc) and the standard deviation (SD) is calculated for each studied heat rate. The obtained results are presented in the Fig.13. The critical temperature seems to be not influenced by the studied W/P mass ratio but this parameter is clearly linked to the heat rate (β). Logically, the more β is, the more the critical temperature is. Such a behavior is directly linked to the thermal ability of the material to adapt its response to the thermal loading (Cp effect).

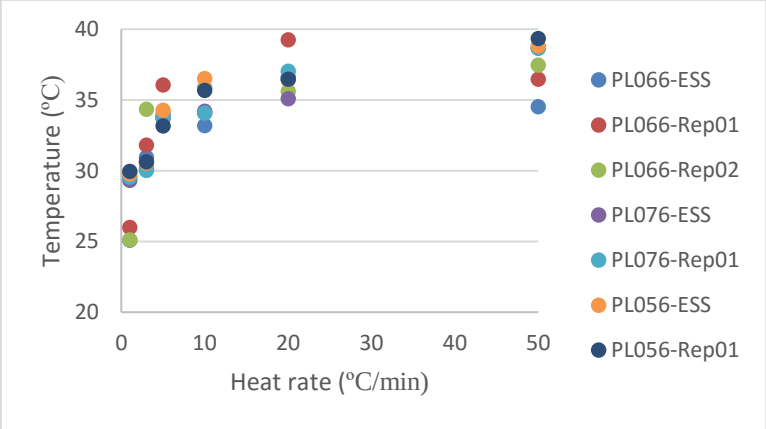

Fig.12 Critical temperature for all water content ratios by heat rate.

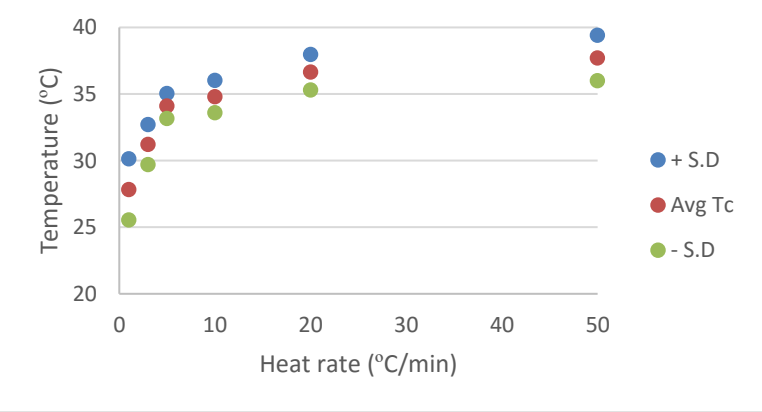

Fig.13 Average critical temperature for all water content ratios at each heat rate.

Thermal dilatation in zone 2 is the effect of the water inside the sample. For each mixing and each thermal test, thermal dilatation coefficient is calculated. Thermal transition between zone 1 and zone 2 and between the zone 2 and zone 3 are avoided to better increase the quality of the calculus and to avoid the effect of the mass transfer. The evolution of the thermal expansion coefficient (β_T) versus the heat rate is presented in the Fig.14. The calculated regression coefficients are presented in the Fig.15 to illustrate the signification of such parameter. R^2 is ranged between 0.9838 and 0.9996. These results show that the studied water to plaster ratio have no real effect. The effect of the heat rate seems to be not constant. Such way is probably

induced by the scale effect and more exactly by the inertial effect. Statistical analysis based on the entire obtained data is conducted. The effect of the W/P ratio is not taken into account.

A histogram of β_T value is performed. The result is presented in the Fig.16. In spite of significant flatness, the tendency described by the histogram is closed to a Laplace-Gauss law. The major mode is equal to 1.496×10^{-5} (1/°C) and the standard deviation is 1.515×10^{-6} (1/°C). Finally, in the present study, we assume the major mode to well represented the average value of the thermal dilatation coefficient.

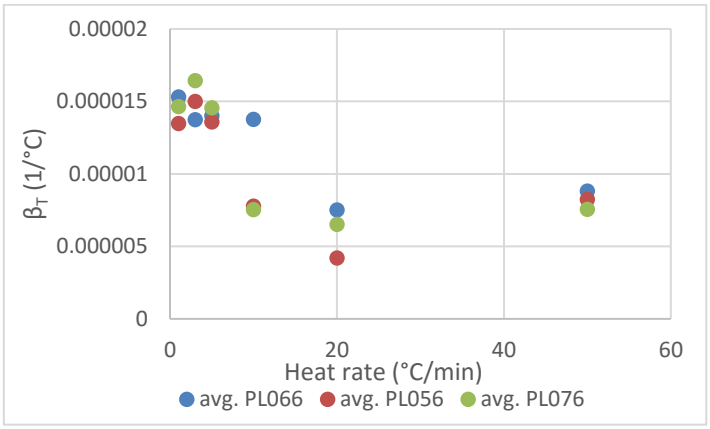

Fig.14 Thermal expansion coefficient behavior between 28ºC to 80ºC

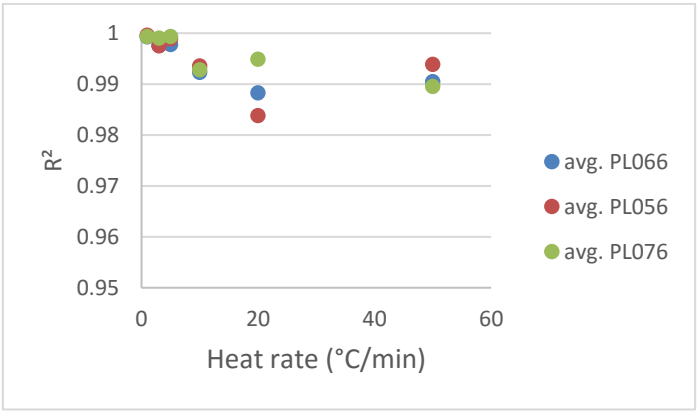

Fig.15 linear regression coefficient behavior between 28ºC to 80ºC

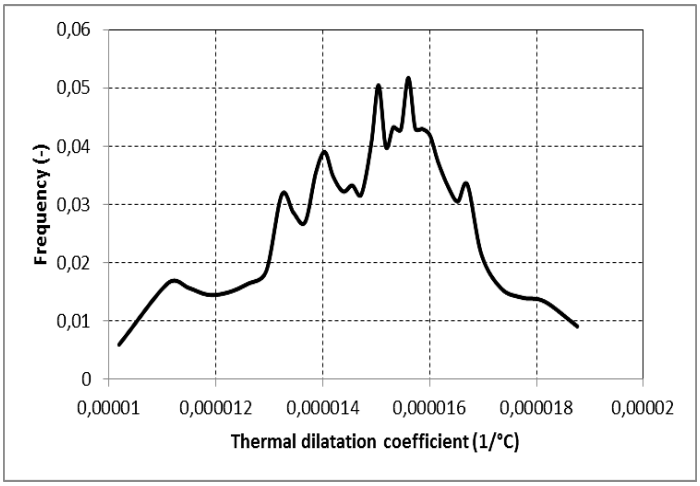

Fig.16 Statistical analysis of the thermal dilatation coefficient. Histogram of the calculated data.

Water to plaster ratio does not seem to have an influence on the duration of dehydration, Fig.17 shows the dilation behavior of the three water ratios on the test of 1ºC/min.

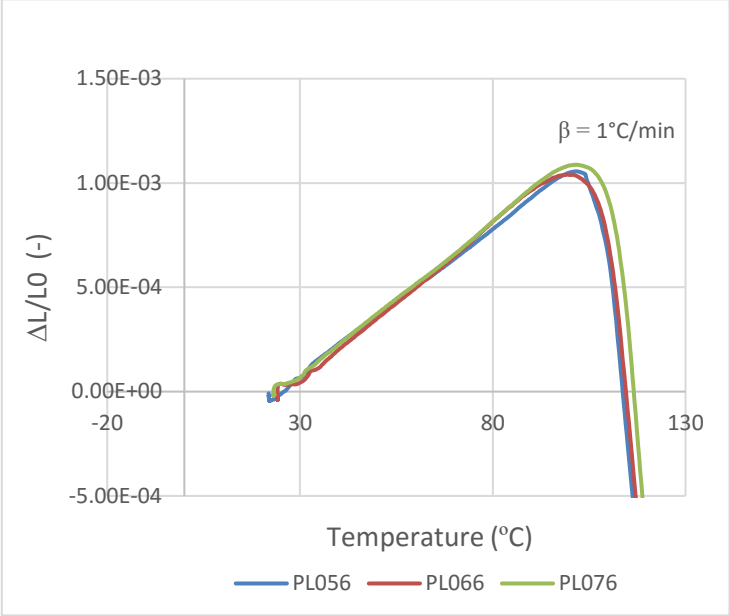

Fig.17 Dilation behavior of plaster in 1ºC/min test with different W/P

In the other hand, the influence of heat rate (β) on the duration of dehydration is noticeable. Duration of dehydration period is measured using temperature difference (ΔT). In fact, such a parameter can be used as a TDA or TGA result. In the present test, the real porous media is analyzed, whereas the samples are often milled in the thermo differential analysis. After unifying the time between dilatometer temperatures data (T_dilato) and thermocouples temperatures data, temperature difference (ΔT) are calculated. Fig.18 presents the relationship between ΔT and T_dilato, from which the value of ΔT is found at the end of the dehydration period. This value is then used to determine the time of dehydration period using Fig.19 which presents the relationship between temperature difference and the experimental time (t*). Table.5 shows the duration of dehydration for each heat rate;

β (°C/min)	1	3	5	10	20	50
ΔT	13	12.62	27.68	52.68	74.26	80.76
t* (s)	10,000	1980	1300	900	540	220
t* (min)	166	33	22	15	10	4
t_{TGA} (s)	6192	2564	1685	992	888	627
t_{TGA} (min)	103	43	28	17	15	10

Table.5 Experimental time for dehydration for each heat rate for plaster of 0.66 W/P

Such a duration is compared to the same duration obtained with thermo gravimetric analyses. A 10 mg samples milled are tested under non isotherm protocol (linear variation of the temperature versus time). Results corresponding to the dehydration period are presented in Fig. 20. Tests are carried out with the same heat rate. For each heat rate, the obtained duration is reported in the table 5. Finally, the obtained results are in good agreement. Scale effect seems to be not significant in term of mass transfer.

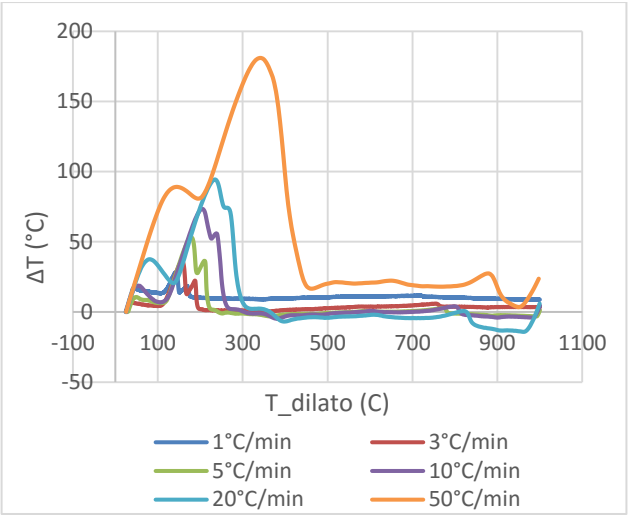

Fig.18 Temperature deference versus T_dilatometer

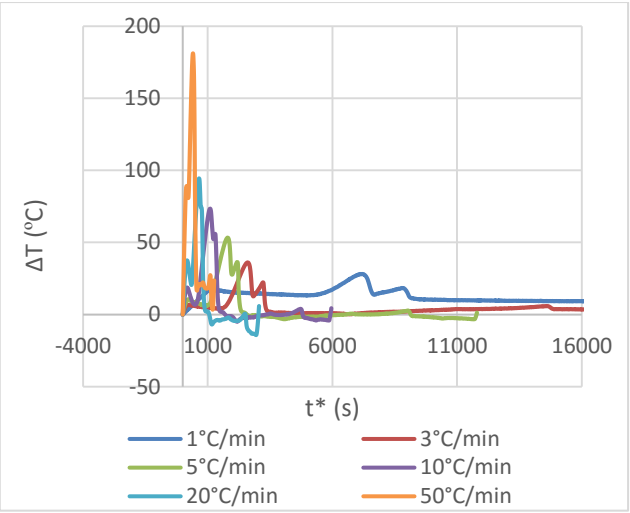

Fig.19 Temperature deference versus experimental time

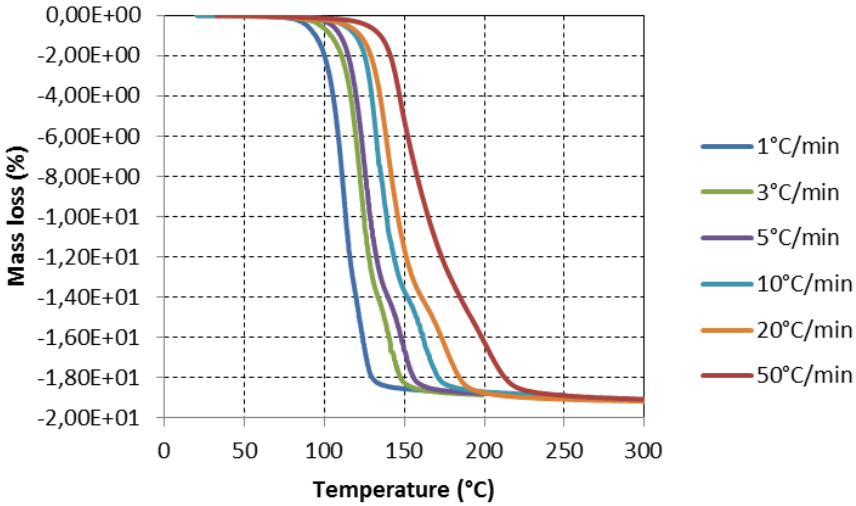

Fig.20 Thermo gravimetric analyses (TGA) of the studied material.

In the limit of the zone 2, reversibility of the phenomena is tested with several samples. Temperature is firstly fixed to increase linearly between room temperature and 60°C. Then thermo strain is registered during the cooling period. Illustration of the good agreement is given in Fig.21.

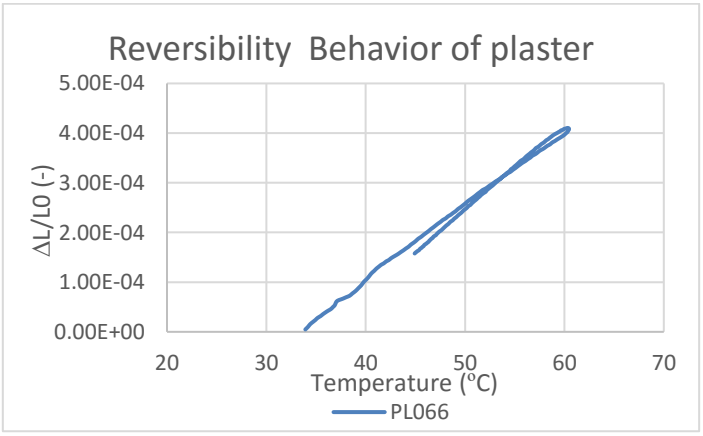

Fig.21 Reversibility behavior of plaster

c. Characterization of the contraction in zone 3

Because of the temperature gradient, the initiation of the dehydration chemical change and the effect of the heat rate, the thermo strain obtained in the zone 3 characterizes mainly a contraction combined with the mass transfer. Analysis of the thermal expansion coefficient (β_T) was done in the zone 3 to test the effect of the mass transfer. It was found that as the heat rate β increases the slop increases see Fig.23. The diminution of the slope indicates the influence of mass transfer. This effect occurs as a result of the dilating-contracting behavior of the plaster composition. With heat augmentation, water inside the sample transfers to the center where it becomes hydrate and dilating, whereas the surrounding parts become dehydrate and contracting. Plus, effect of the studied water to plaster mass ratios have no significant effect.

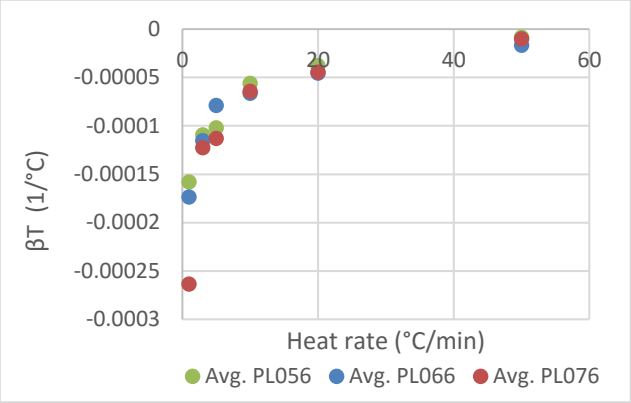

Fig.23 Thermal expansion coefficient behavior of plaster in zone 3

d. Characterization of the contraction in zone 5

The zone 3 and the zone 5 are separated by a plateau. Between these two zones, no chemical changes are noticeable. The zone 5 is induced by the crystal morphology change. No mass transfer is associated to this chemical change. Analysis of the thermal expansion coefficient (β_T, parameter of the zone 5) was done and presented in the figure Fig.24. This slope pattern indicates that globally the contracting process in zone 5 is independent and does not get influenced by the heat rate β. This slope presents the reorganization of system crystals from Anhydrite III to Anhydrite II (exothermic reaction). Plus, the studied water to plaster mass ratios have no noticeable effect on the expansion coefficient.

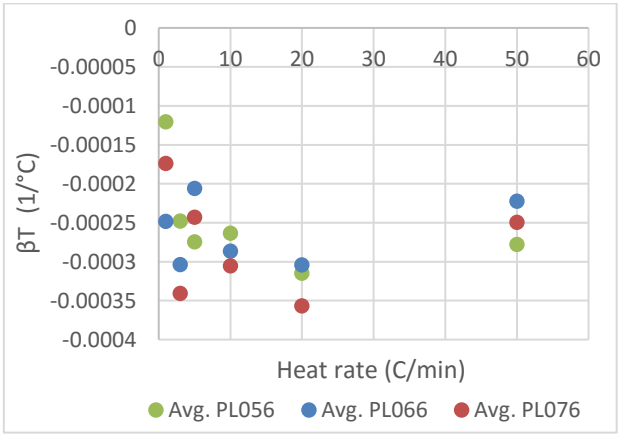

Fig.24 Thermal expansion coefficient behavior of plaster in zone 5

e. Analysis of zones 6, 7 and 8

After the achievement of the Anhydrite III to Anhydrite II chemical change, SEM analyses show the mechanical damages development of the crystals needles with increasing temperature. At high temperature sintering characterize the chemical change of the material. Previous works [16] help us to characterize the material densification and porosity decreasing. As a consequence, the measured thermo strains characterize mainly a contraction behavior. Nevertheless, such main behavior seems to be combined with the calcite chemical change (Zone 7).

The studied plaster shows four phases changes from 25°C to 1000°C each with a chemical reaction [5]:

Gypsum → hemihydrate	$CaSO_4.2H_2O \leftrightarrows CaSO_4.0{,}5H_2O + 1{,}5H_2O$
Hemihydrate → anhydrite III	$CaSO_4.0{,}5H_2O \leftrightarrows \gamma\text{-}CaSO_4 + 0{,}5H_2O$
Anhydrite III → anhydrite II	$\gamma\text{-}CaSO_4 \leftrightarrows \beta\text{-}CaSO_4$
Calcite → Calcium Oxide	$CaCO_3 \rightarrow CaO + CO_2$

f. Thermo-rheological behavior representation using master curves

In the previous section, the effect of the heat has been presented especially when the chemical changes of the material induce a mass transfer and as a consequence, induced identified parameter is linked to the heat rate (because of the thermal transfer induced by the temperature gradient). Nevertheless, we achieve the thermo strain analysis with an attempt of the global representation of the effect of temperature by mean a master curve. Unifying representation for plaster (W/P 0.66) was done by slipping the graphs of different heat rates with 1ºC/min as a reference graph, in order to present a one master solution for the dilation contraction behavior see Fig.26 and Fig.27.

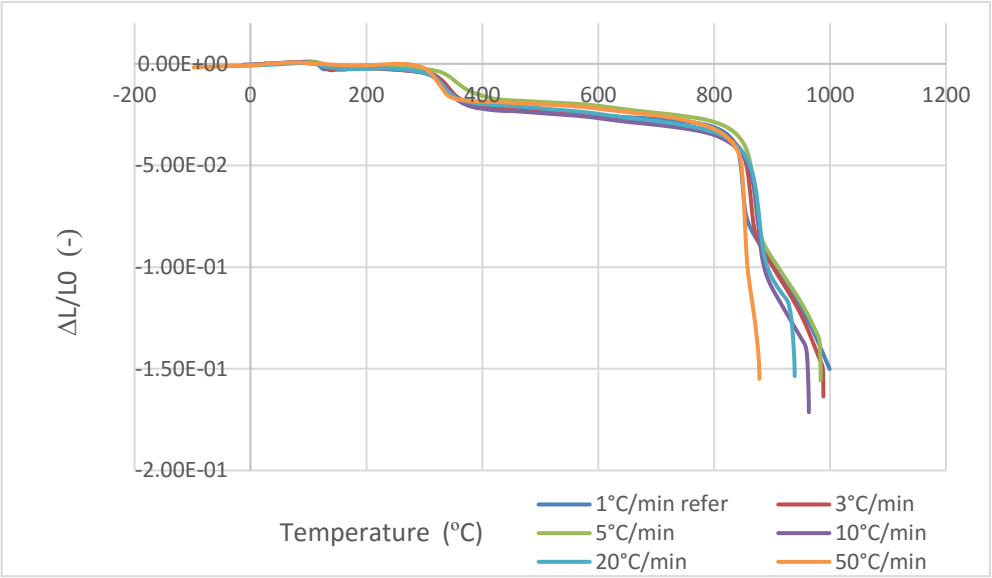

Fig.26 Master curve of the first test of plaster with water content ratio of 0.66 at all heat rates.

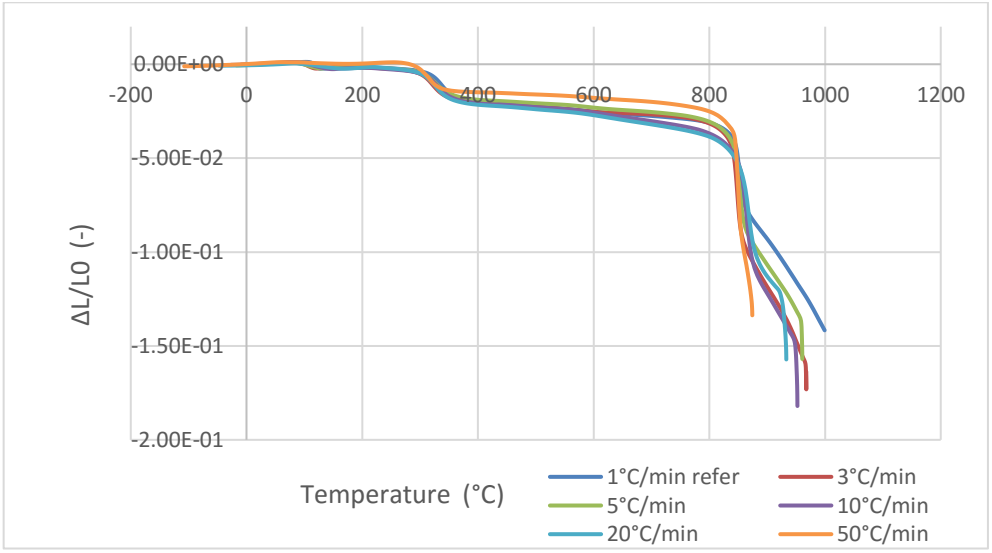

Fig.27 Master curve of the first repetition of plaster with water content ratio of 0.66 at all heat rates.

These curves allow to have a general idea on the overall effect of heat rate on the behavior of plaster. The others water content ratios master curves can be found in the Appendix.

Ch.V) RHEOLOGICAL BEHAVIOR IMPROVEMENT

To improve the plaster behavior, the chemical composition is changed by adding silica fume. The behavior of plaster with silica fume composition contracts 20% less than plaster composition only, see Fig.28.

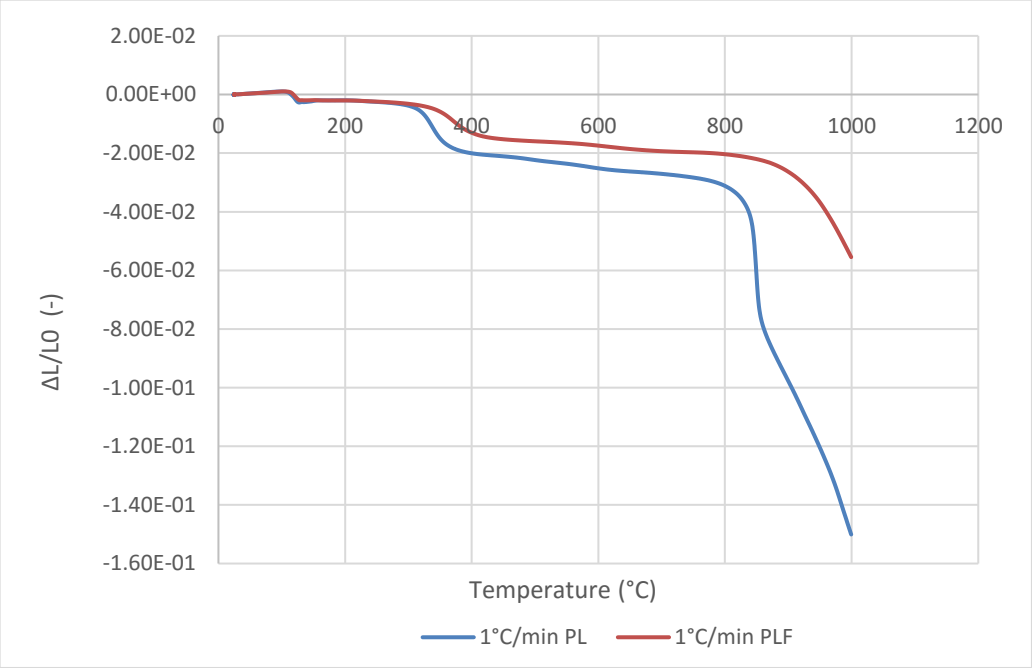

Fig.28 Comparison between plaster (PL) and plaster with silica fume (PLF) compositions at 1°C/min

CONCLUSION

The work done during this project has contributed to a better understanding of the plaster thermo rheological behavior under severe thermal loading -fire like conditions- using the standard ISO 834 fire curve. Thermal, hydrous, chemical and mechanical behavior (THCM) is investigated using thermo dilatometer on cylindrical samples of β- hemihydrate plaster. Three different water to plaster ratios and six different heat rates were used to study their influences on THCM.

General dilatation behavior is divided into eight zones (Fig.10), starting with a temperature yield period (zone 1). The dilatation process is noticed in (zone 2) governed by the water content. Contractions start after dehydration in (zone 3), the limit of irreversibility found to be at (zone 4). Chemical transformation from Anhydrite III to Anhydrite II occurring at (zone 5). For the rest of the zones (6, 7 and 8), the contraction is in accordance with the chemical change of the Anhydrite II to Anhydrite I and it is combined with the dilatation of the CO_2 release during the chemical change of the calcite.

The critical temperature seems to be not influenced by the studied water to plaster mass ratio but it is clearly linked to the heat rate (β), the more β is, the more the critical temperature is. Water effects the dilatation behavior of the dehydration in zone 2, however W/P ratio does not have an influence on the duration of dehydration (Fig.17). In the other hand, the heat rate (β) has an influence on the duration of dehydration, this was realized after temperature deference analysis using thermocouples (Table.5).

The studied water to plaster mass ratios have no noticeable effect on the expansion coefficient. In the other hand, heat rate β has also an influence on the thermal expansion coefficient β_T. It was found that as the heat rate β increases the slope increases (Fig.23). This evolution of the slope indicates the influence of water mass transfer in the tested sample. Analysis of the thermal expansion coefficient β_T in zone 5 was done (Fig.24) indicates that globally the contracting process is independent and does not get influenced by the heat rate β. This slope presents the reorganization of system crystals from Anhydrite III to Anhydrite II.

At the end of this project, a global representation of the effect of temperature by mean a master curve was presented in (Fig.26). These curves allow to have a general idea on the overall effect of heat rate on the behavior of plaster. One method was mentioned to improve the plaster behavior by adding silica fume to the chemical composition which helped in 20% reduction on contraction.

REFERENCES

[1] F.Iucolano, D.Caputo, F.Leboffe, B.Liguori, " Mechanical behavior of plaster reinforced with abaca fibers ". ScienceDirect, Construction and Building Materials 99 (2015) 184–191

[2] J. Karni, E.Y. Karni, “Gypsum in construction: origin and properties, Mater. Struct”. 28 (2) (1995) 92–100.

[3] Eurogypsum aisbl - Rue de la presse 4 - 1000 Brussels – Belgium , (2011). < http://www.eurogypsum.org/about-gypsum/the-european-plaster-and-plasterboard-industry/the-european-industry-overview/>.

[4] J. L. LEWANDOWSKI, Materials for casting moulds, Ed. Akapit, Cracow (1997).

[5] A. ROJO, ‘’Etude de la structuration et du comportement de matériaux à base de gypse sous condition incendie’’. INSA Rennes - LABORATOIRE LGCGM, 2013.

[6] N.B.Singh, B.Middendorf, ‘’Calcium sulfate hemihydrate hydration leading to gypsum crystallization’’. 53, 57-77, 2007.

[7] C. Bezou, “Etudes des caractéristiques cristallographiques, thermodynamiques et microstructurales des produits de déshydratation du gypse,”. Thèse de doctorat, UR des Sciences et Techniques, Université de Bourgogne, 1991.

[8] H. Lehmann, Tonind. Ztg. 91 (1967) 6.

[9] S. Follner, A. Wolter, A. Preusser, S. Indris, C. Silber, H. Follner, Cryst. Res. Technol. 37 (10) 1075, 2001.

[10] M.Nadolski, Z.Konopka, M.Lagiewka, A.Zyska, “Dilatometric examination of moulds with plaster binder. Department of Foundry”. Technical University of Częstochowa, Volume 11 P : 83-86, 2011.

[11] Techniques de l’ingénieur, Daligand D. Plâtre. Editions T.I., 2014.

[12] N.Payraudeau, S.Meille, J.Chevalier, E.Maire and J. Adrien, " In situ observation of plaster microstructure evolution during thermal loading". Université de Lyon. Wiley Online Library. DOI : 10.1002/fam. 2357, 2016.

[13] D. Quénard, J.-P. Laurent, and H. Sallée, “Influende de la teneur en eau et de la tempértaure sur les paramètres thermiques du plâtre,”. Revue Générale de Thermique Française, vol. 291, pp. 137-144, 1986.

[14] S. V. Shepel, K. G. Wakili, and E. Hugi, “Vapor convection in gypsum plasterboard exposed to fire: numerical simulation and validation,”. Numerical Heat Transfer Part a-Applications, vol. 57, no. 12, pp. 911-935, 2010.

[15] PROMAT INTERNATIONAL N.V. Fire Protection, Cellulosic curve < http://www.promat-tunnel.com/en/advices/fire-protection/fire%20curves>

[16] A. ROJO, Y. MELINGE, O. GUILLOU, “Kinetics of internal structure evolution in gypsum board exposed to standard fire”, Journal of Fire Sciences, 31(5), pp 395-409, 2013.

APPENDIX

Master curves of water to plaster ratios of 0.56 and 0.76:

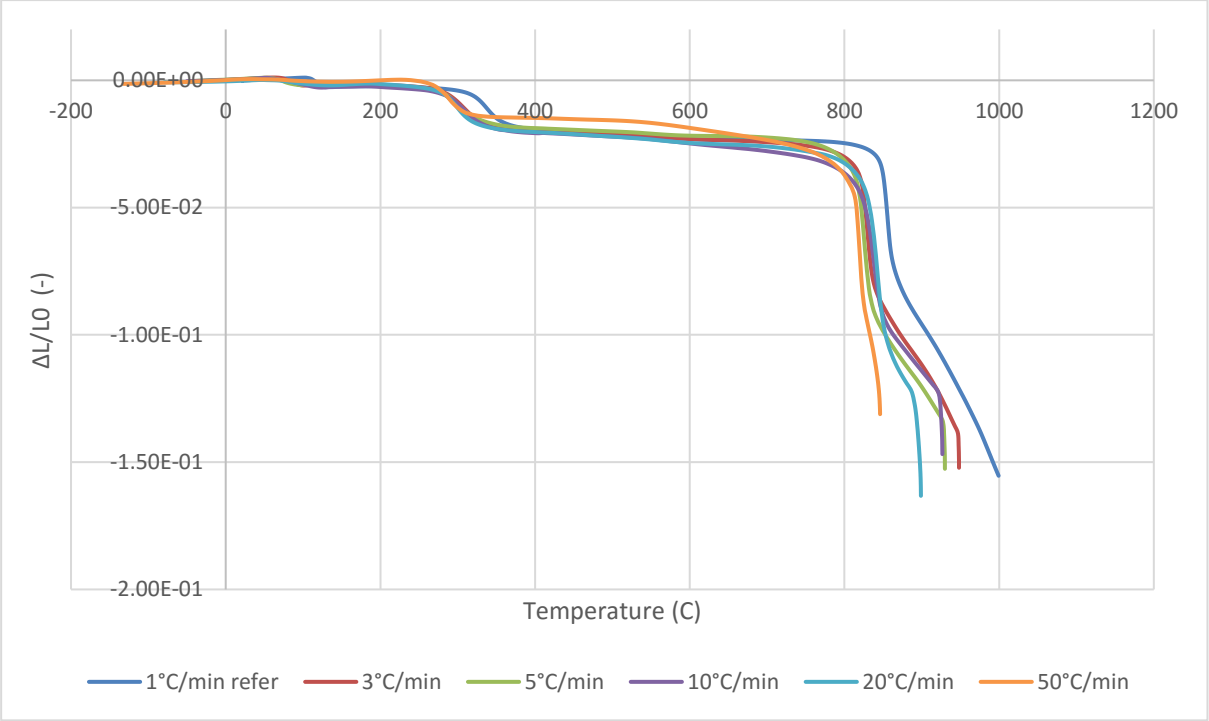

Master curve of the first test of plaster with water content ratio of 0.56 at all heat rates.

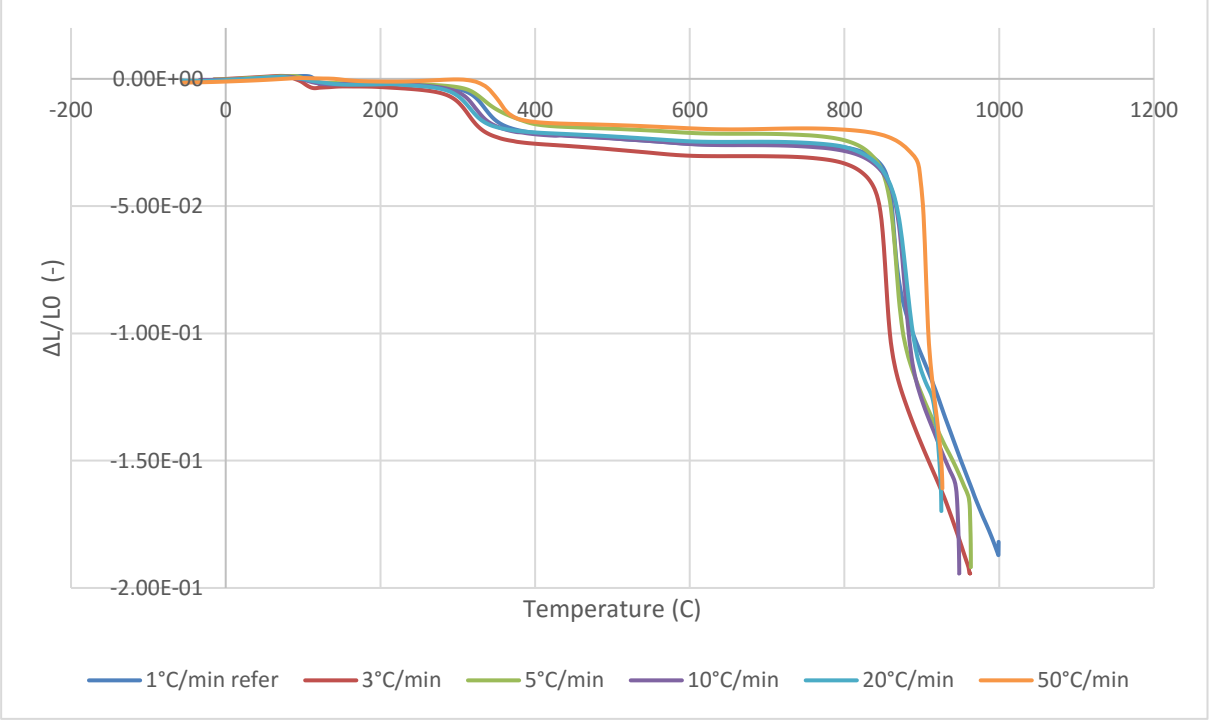

Master curve of the first test of plaster with water content ratio of 0.76 at all heat rates.